

Transcription Profile of Kaposi's Sarcoma-associated Herpesvirus in Primary Kaposi's Sarcoma Lesions as Determined by Real-Time PCR Arrays¹

Dirk P. Dittmer²

Department of Microbiology and Immunology, The University of Oklahoma Health Sciences Center, Oklahoma City, Oklahoma 73104

Abstract

Kaposi's sarcoma (KS) is the signature pathology of AIDS. KS-associated herpesvirus (KSHV/HHV-8) is causally linked to KS. Here, we report the first complete profile of KSHV transcription in primary KS lesions using a novel, real-time PCR array. The KSHV latency I mRNAs [latency-associated nuclear antigen (LANA)/orf73, v-cyclin/orf72, and v-FLIP/orf71] were invariably present in all biopsies. Yet, viral lytic mRNAs were detectable in only a subset of tumors. Interestingly, there was a difference in the expression pattern of the viral IFN-regulatory factors (vIRFs) encoded by KSHV. The vIRF-1/K9 clustered with LANA in KS, in contrast to its homologue, vIRF-3/LANA-2, which is transcribed only in KSHV-associated lymphomas. This suggests that the various vIRFs encoded by KSHV are important for KSHV latency as well as KS tumorigenesis and that their redundancy may be explained in part by a tissue-specific regulation. Clinical KSHV transcriptional profiling as described here will prove useful for the identification of KS tumor markers for diagnosis and as potential drug targets. Stratification by KSHV lytic transcription can identify lesions with a high percentage of lytically infected cells, which may respond to antiviral drugs.

Introduction

In 1981, KS³ was recognized as the signature pathology for AIDS (reviewed in Ref. 1). Although highly active antiretroviral therapy led to a decline of AIDS-related KS in the United States, mounting failure rates in patients on highly active antiretroviral therapy (primarily due to noncompliance) suggest that KS will represent a health problem for years to come. Classic KS predates the HIV/AIDS epidemic and was first described in 1872 as a disseminated sarcoma of the skin. KS is endemic in sub-Saharan Africa. Here, transmission of KSHV proceeds from mother to child before puberty, and KS is fatal. Today's widespread HIV-1 coinfection has dramatically increased KS incidence rates in this area. Prevalence levels for anti-KSHV antibodies reach 30% in some South African HIV patients, and childhood KS has become the most common neoplasm in many parts of the African continent. Lastly, KS has been documented in organ transplant recipients, in whom it comprises an estimated 3% of tumors, particularly in regions of high KSHV prevalence, such as Southern Italy, Turkey, and Saudi Arabia.

KSHV/HHV-8 DNA can be found in every KS lesion. Every KS

tumor cell expresses at least one viral protein: the LANA/orf73 (2). Antibodies to LANA exist in virtually all HIV-infected as well as non-HIV-infected KS patients, and other viral antigens have also been identified as the targets of this response. Prospective, longitudinal studies found that increases in peripheral blood viral load as well as KSHV-specific antibody titers precede the onset of disease and correlate with increased risk for KS. In addition, two lymphoproliferative disorders, primary effusion lymphoma (PEL) and multicentric Castlemans disease (MCD), are associated with KSHV (3, 4). These observations imply (a) that KSHV viral oncogenes are required for KS development and (b) that the identification of these viral genes may provide highly specific tumor markers and/or rational intervention targets for KS therapy.

We and others previously analyzed KSHV transcription in PEL-derived cell lines (5–7). By and large, these experiments confirmed the transcriptional patterns that were previously assembled for individual KSHV latent and lytic genes in KS and KSHV-associated PEL, but it is conceivable that viral gene expression differs between KSHV-associated B-cell lymphoma and KS, a KSHV-associated sarcoma of endothelial cell lineage. Thus far, however, the scarcity of material has prevented the genome-wide transcriptional analysis of KSHV in primary KS lesions. By applying a novel, real-time quantitative RT-PCR array (5), we were able to query the transcription profile of viral genes across the entire KSHV genome in 21 primary KS biopsies. The KSHV latency locus, encompassing LANA/orf73, the v-cyclin/orf72, and v-FLIP/orf71, was consistently transcribed in all 21 KS tumors, as was the vIRF K9/vIRF-1.

Materials and Methods

Tumor Samples. Twenty-four specimens were obtained from the ACSB.⁴ Written consent was obtained from all patients before submission of material to the bank. Use of the samples was reviewed and approved by the institutional review board of the University of Oklahoma Health Sciences Center. The specimen cohort reflects historical submissions to the ACSB. The mean age of patients was 48 ± 9 years, 2 individuals were female, and 21 were male. Seventy-four percent were HIV positive, 4% were HIV negative, and HIV status was not available for 22%. Three biopsies did not yield a signal for GAPDH, a housekeeping mRNA, and were excluded from the analysis.

RNA Extraction and Real-Time, QPCR. RNA was isolated as described previously (5) using RNazol (Tel-Test, Inc., Friendswood, TX). Polyadenylated mRNA was prepared using dT-beads (Qiagen Inc., Valencia, CA) and reverse-transcribed using Superscript-II reverse transcriptase (Life Technologies, Inc., Rockville, MD), according to the manufacturers' recommendations. The KSHV real-time QPCR array has been described previously (5). The final PCR reaction contained 2.5 μl of primer mix (final concentration, 166 nM), 7.5 μl of 2× SYBR PCR mix (Applied Biosystems, Foster City, CA), and 5 μl of sample. To guard against contamination and handling errors, all real-time QPCR reactions were assembled in a segregated clean room using a CAS-2000 robot (Phoenix Inc., Hayward, CA) with 0.1 μl accuracy, liquid level sensing, and filtered pipette tips. Real-time PCR was performed using an ABI PRISM5700 machine (Applied Biosystems) and universal cycle conditions.

⁴ <http://acsb.ucsf.edu/>.

Received 12/16/02; accepted 3/19/03.

The costs of publication of this article were defrayed in part by the payment of page charges. This article must therefore be hereby marked *advertisement* in accordance with 18 U.S.C. Section 1734 solely to indicate this fact.

¹ Supported by a contract from the AIDS Malignancy Consortium and NIH Grants EB000983 and CA97951.

² To whom requests for reprints should be addressed, at Department of Microbiology and Immunology, The University of Oklahoma Health Sciences Center, 940 Stanton L. Young Boulevard, Oklahoma City, OK 73104. Phone: (405) 271-2690; Fax: (405) 271-3117; E-mail: dirk-dittmer@ouhsc.edu.

³ The abbreviations used are: KS, Kaposi's sarcoma; KSHV, KS-associated herpesvirus; vIRF, viral IFN-regulatory factor; LANA, latency-associated nuclear antigen; PEL, primary effusion lymphoma; RT-PCR, reverse transcription-PCR; GAPDH, glyceraldehyde-3-phosphate dehydrogenase; ACSB, AIDS and Cancer Specimen Bank; QPCR, quantitative PCR; NTC, nontemplate control. CT, cycle threshold; MCD, multicentric Castlemans disease.

Statistical Analysis. Hierarchical clustering was performed as described previously (8). All samples were normalized to GAPDH, centered by median of gene, normalized to ± 1 , and ordered by hierarchical clustering (prior k-tuple sort or self-organizing maps did not change the outcome). Calculations were performed using Excel (Microsoft Inc., Redwood, WA) and SPSS (SPSS Science, Chicago, IL). Two types of normalization were applied: type I normalization relative to median for each gene yielded δ CT (henceforth abbreviated δ); and type II normalization relative to the reference gene GAPDH yielded Δ CT (henceforth abbreviated Δ). The latter eliminates differences due to variation of the overall input cDNA concentration. During type I normalization, only CT values of a single primer pair are compared with each other. Hence, amplification efficient differences between primer pairs do not enter the calculation. In contrast, type II normalization compares two different primer pairs, such as those for gene A and gene GAPDH, with associated, possibly different, amplification efficiencies k_A and k_{GAPDH} . After both normalizations were applied successively, we obtained $\delta\Delta$ CT (unfortunately, current literature uses Δ CT for type II and $\Delta\Delta$ CT to denote the outcome after both normalizations,⁵ which masks the different properties of the two operations). Because we performed clustering in log-space on the initial CT values rather than interpolated mRNA levels, only a linear term is subtracted from each sample, which did not impact the rank order between tumor samples. Furthermore, we determined the amplification efficiency for each primer pair in the array (data not shown). The mean amplification efficiency E was 1.94 ± 0.12 ($n = 91$) for the entire array, and the associated SE was 6%, which is well below the biological variation that is associated with clinical specimens.

Results

Real-Time, Quantitative RT-PCR Arrays. Real-time QPCR has been established as a powerful, specific, and extremely sensitive tool to quantify DNA, such as encountered in viral load assays, or—after reverse transcription—RNA. Real-time QPCR measures the amount of product at each cycle of PCR. Hence, the exponential phase of the amplification reaction can be visualized and used for quantification. The standard readout of various instruments and chemistries, which are currently in use for real-time QPCR, is expressed as CT (also written as C_t). The CT value denotes the cycle number at which sufficient PCR product has accumulated to cross a user-defined threshold. Lower CT values indicate higher target concentrations. CT values can be related to absolute or relative target concentrations by using an external standard curve or generally accepted approximations (9–11). The analysis presented here relies on hierarchical clustering (8) of the initial CT data rather than interpolated mRNA levels. This excludes any potential bias, which might be introduced by different amplification rates for different primer pairs. Rather than quantifying any one particular mRNA at a time, we used a real-time quantitative RT-PCR array, which queries the entire KSHV transcriptome (5). This QPCR array delivers the same information as comparable hybridization-based DNA arrays (data not shown) but uses only a fraction of input material, which allowed us to sample clinical, primary KS biopsies. Because of the inherent sensitivity of PCR, no generalized enhancement step (such as T7 amplification or primer switching) was necessary before PCR with gene-specific primers. This eliminated any bias against rare mRNAs, which may otherwise be inappropriately amplified during enhancement and skew our interpretation of the data. In summary, our assay is both quantitative and qualitative.

To explore the KSHV transcription profile in primary KS tumors, we obtained 24 KS biopsies from the ACSB. However, we excluded three of these samples from further analysis because the GAPDH control could not be amplified from these three samples. The panel of 21 samples was collected at different institutions from a number of KS patients before their enrollment into clinical trials. At the time, these samples represented all cryopreserved KS samples that were available

to the wider research community. Cryopreserved samples are still the optimal source for reliable mRNA extraction. The small sample size (2×2 -mm punch biopsies) and substantial RNase activity in the highly vascularized KS lesions thwarted prior attempts to investigate KSHV transcription using hybridization-based arrays but presented no obstacle for the RT-PCR-based array described here.

The Total Levels of LANA mRNA Correlate and Are Indicative of the Amount of KS Tumor Cells in a Biopsy. Clinical biopsies can vary considerably with regard to how many tumor cells and how many nontumor cells are present. To identify the most sensitive and specific probe in our array, which could identify the presence of KSHV-infected tumor cells, we compared tumor with NTC control. None of the PCR primers yielded any specific product when analyzed by agarose gel electrophoresis (data not shown). However, SYBR-green-based real-time QPCR is much more sensitive compared with gel-based analysis, and nonspecific products (such as primer dimers) may yield a signal at late cycles. Fig. 1A plots the mean CT values of 21 KS biopsies for each primer pair in the KSHV array over the CT value of the NTC reactions. None of the primer pairs in the array yielded any signal of the NTC prior to 30 cycles, which is the upper

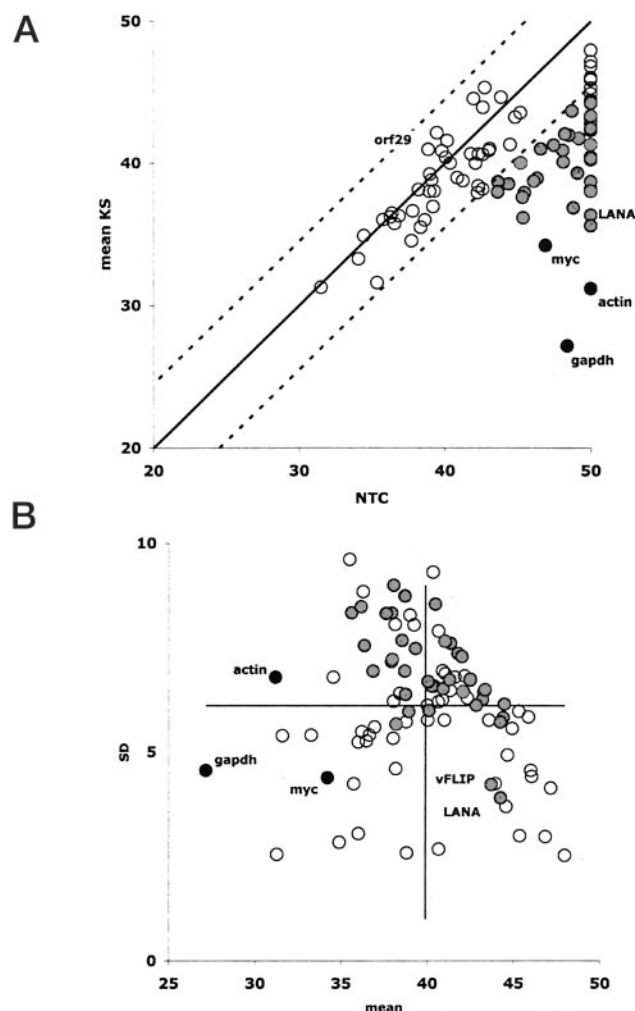


Fig. 1. A, the mean CT value for each primer pair obtained after amplification of KS tumor-derived cDNA pools ($n = 21$) is plotted on the vertical axis, and the CT of NTC is plotted on the horizontal axis. Cellular mRNAs are highlighted by ●, mRNAs with a mean CT $> 1 \times$ SD above NTC are highlighted in gray. Also shown is the 45° equivalency line (solid line) as well as the SD for GAPDH in all KS tumors (dashed line). B, the SD for each primer pair is plotted on the vertical axis, and the mean CT is plotted on the horizontal axis. Cellular mRNAs are highlighted by ●, mRNAs with a mean CT $> 1 \times$ SD above NTC are highlighted in gray. Also shown are the mean SD and the average mean CT for all KS tumors.

⁵ ABI user bulletin P/N4303859.

limit for conventional PCR. Eighty-eight of 91 primer pairs (97%) did not yield a signal from the NTC prior to 35 cycles, and 74 of 91 primer pairs (81%) yielded no signal in the NTC reaction even after 40 cycles of PCR. However, rather than choosing a single cutoff value across the entire array, Fig. 1A allowed us to establish significance and sensitivity limits for each primer pair based on the individual NTC reaction. Primer pairs below the 45° equivalency line (Fig. 1A) showed no amplification in the NTC reaction (*horizontal axis*) but showed a significant signal for KS samples (*vertical axis*). For example, the mRNA for GAPDH was present at the highest level (mean $CT_{KS} = 27 \pm 6$ compared with mean $CT_{NTC} = 48$) in all samples (Fig. 1A, ●). Based on the GAPDH SD for KS tumors (SD = ± 6), GAPDH mRNA was 3× the SD more abundant in KS samples compared with the NTC reaction, demonstrating the range of our RT-PCR assay. Assuming ideal amplification efficiency, GAPDH mRNA levels were $2^3 \times 17 = 10^{15}$ -fold above background. Three KS samples that did not yield appreciable GAPDH mRNA levels were excluded from further analysis. Other cellular mRNAs *e.g.*, actin and myc (Fig. 1A, ●), exhibited similarly high levels (as indicated by low mean CT values) because these are also transcribed in every cell.

KSHV-specific mRNAs were also detected in the KS tumor biopsies at significant levels (Fig. 1A, *gray circles*). Primers specific for LANA/orf73 mRNA yielded significant amplification in all tumors. The levels for LANA mRNA were calculated to be $2^{1.5 \times 7} = 1000$ -fold above background of the NTC reaction. This is consistent with prior *in situ* analysis for LANA, which showed that LANA protein is expressed in every KS tumor cell (2, 12). LANA mRNA was less abundant than GAPDH mRNA for two reasons: firstly, not all cells in the KS biopsy are KS tumor cells. KSHV-negative infiltrating lymphocytes as well as surrounding normal tissue are also present in the biopsy. Secondly, on a per cell basis, GAPDH mRNA is more abundant than LANA mRNA, as shown by real-time QPCR analysis in BCBL-1 cells (5, 13).

Many KSHV gene-specific PCRs did not differ significantly in their mean CT for the KS samples as compared with the NTC (Fig. 1A, ○). This could be because a particular primer pair was not sensitive enough or because the corresponding mRNA was not present at high enough levels to be detected. The latter possibility is more likely because this real-time QPCR is capable of detecting all KSHV mRNAs in as little as 5000 KSHV-infected BCBL-1 cells undergoing lytic reactivation (5). In BCBL-1 and other PEL cell lines, every single cell is infected with KSHV, whereas only the endothelial cells in the KS lesion are infected with KSHV. The result for the KSHV lytic mRNA orf26 illustrates this observation (Fig. 1A, ○). Based on *in situ* hybridization assays, 1% of KS tumor cells transcribe lytic mRNAs (12). This percentage, however, varies widely between individual samples, and with KS stage (nodular, plaque, patch). Hence, the mean CT_{KS} values for orf29 and other lytic mRNAs did not differ significantly from the CT_{NTC} of the control reaction. Importantly, this does not imply that lytic KSHV viral mRNAs are not transcribed in KS tumor samples or that their expression is not required for the development of KS but rather that the detection of these lytic mRNAs is below the sensitivity of an analysis of means. This is illustrated in Fig. 1B. Here, the SD_{KS} , an indicator of variability within our sample collection, is compared with the mean CT_{KS} for all samples. GAPDH and myc exhibit a low SD and are highly abundant (low mean CT_{KS} ; Fig. 1B, ●) because these cellular mRNAs are transcribed in all cells. LANA and v-FLIP also exhibit a low SD because they are transcribed in each KS sample, but at a lower level (high mean CT_{KS} , Fig. 1B, *gray circles*) compared with GAPDH. The other KSHV mRNAs fall into two classes: (a) mRNAs that were present at such low levels that their mean CT_{KS} did not differ significantly from the NTC (○); and

(b) mRNAs that were present at a level significantly above NTC (*gray circles*), but at very different levels in different samples (high SD).

Differential Transcription Profiles of KSHV Latent and Lytic mRNAs in KS. To gain a more detailed view of KSHV transcription in individual KS tumors and to increase the power of our investigation, we performed cluster analysis of the individual real-time QPCR data (see “Materials and Methods” for details). The three cellular genes in the array, GAPDH, actin, and c-myc, group together (see Fig. 2, *yellow highlight*). This is expected because these three genes signify the amount of total mRNA in each sample. Because of our normalization algorithm (see “Materials and Methods”), the difference $\Delta_{LANA} = CT_{LANA} - CT_{GAPDH}$ signifies the fraction of KSHV-infected cells in each biopsy. It varies widely from biopsy to biopsy with mean (Δ_{LANA}) = 7.75 ± 7.40 , indicative of the fact that individual biopsies contain more or less tumor cells. Hence, the amount of LANA mRNA serves as a marker for KSHV-positive cells and can be used to quantify the amount of KSHV-infected tumor cells in a biopsy. The LANA mRNA level provides an important yardstick for further analysis because the levels of other KSHV latent mRNAs or of cellular mRNAs that are regulated by LANA should correlate with the level of LANA mRNA, whereas levels of lytic mRNAs should not. KSHV lytic mRNAs correlate with the fraction of KS tumor cells undergoing lytic replication, rather than the total fraction of KSHV-infected cells that is measured by LANA. This idea is described in more detail in below.

KSHV mRNAs were divided into two clusters: an upper group and a lower group. The KSHV latency I mRNAs encoding LANA, v-cyclin, and v-FLIP were queried by multiple primers across the locus: lat273F, 73-5'-UTR, 71primer2, Taq-F4, orf72f1 (5). These primers all grouped together [mean of all pairwise Pearson correlations, 0.6 ± 0.1 ($n = 10$); Fig. 2, *red highlight*]. This is consistent with *in situ* observations, which show LANA and v-cyclin to be expressed in all KS tumor cells as well as in all PEL cells (2, 12). Other KSHV mRNAs clustered with LANA as well. However, close inspection revealed that the corresponding primers did not yield a signal above NTC in any of the KS samples. Hence, their transcription pattern is uniform, namely background, across the panel, which led to their grouping with the uniform highly transcribed latency cluster. Only K9/vIRF-1 mRNA was present at significant levels in all KS tumors, which is evidenced by its clustering with LANA (see Fig. 2, *blue highlights*). This establishes K9/vIRF-1 as latent mRNA in KS tumors. It extends an earlier report, which mapped a latency-specific start site for K9/vIRF-3 in PEL 84 bp upstream of a second, lytic cycle-specific start site (14). By comparison, LANA-2/vIRF-3 (15, 16) did not cluster with this group, even though LANA-2/vIRF-3 groups with LANA in terms of its nonresponsiveness to 12-O-tetradecanoylphorbol-13-acetate induction in PEL (5). Thus, the vIRFs represent a group of homologous, redundant KSHV latent genes that are differentially regulated between different KSHV-associated tumor types.

What unites the other KSHV genes (Fig. 2, *top panel*)? These (mostly lytic) mRNAs were not present in all tumors. Here, the median (Fig. 2, *bottom panel, black*) indicates the absence of any mRNA. The apparent less than median levels (Fig. 2, *bottom panel, red shades*) result from normalization to varying GAPDH levels for each tumor samples. Only tumor samples that showed increased mRNA levels (Fig. 2, *bottom panel, blue shades*), as compared with the median, transcribe detectable levels of lytic mRNAs. KSHV lytic mRNAs could be amplified from these tumor samples because the fraction of KS tumor cells undergoing lytic replication was substantial. This is best illustrated by pairwise comparison. Fig. 3 plots CT values for individual genes relative to GAPDH. As shown in Fig. 3A, the level of c-myc mRNA correlated highly with the level of GAPDH

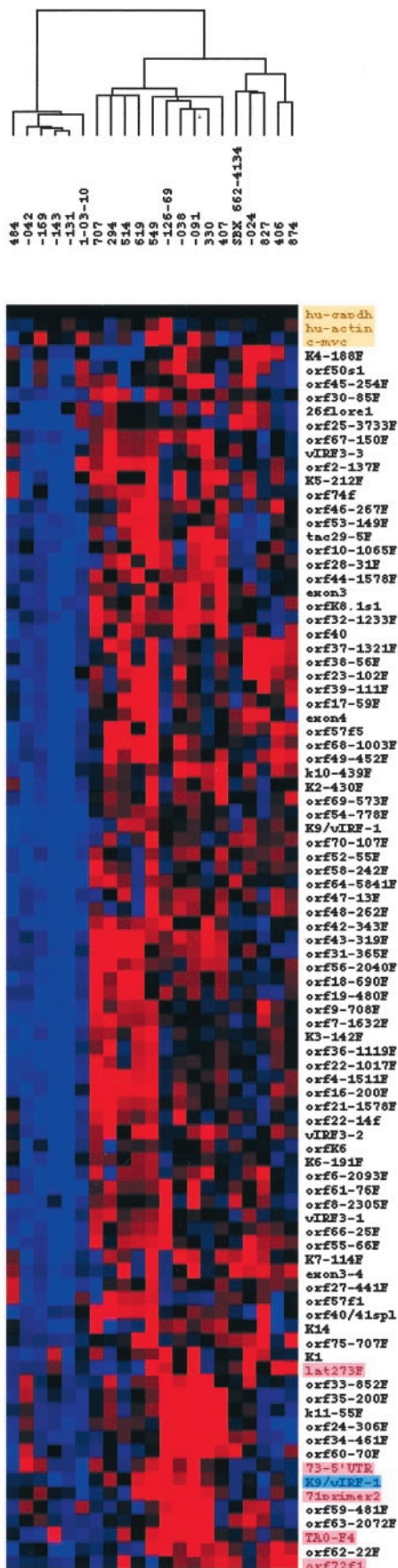


Fig. 2. Treeview representation of hierarchical cluster analysis. Red shading indicates decreased levels relative to the median (black), and blue shading indicates increased levels relative to the median on a logarithmic scale.

mRNA for each tumor sample ($R^2 = 0.7834$, $m = 0.85$). Actin levels did so much less ($R^2 = 0.1357$, $m = 0.55$), which is consistent with published reports that discredit actin as a uniform standard for mRNA normalization (17). Fig. 3B compares the data for orf71/v-FLIP and orf72/v-cyclin to GAPDH. The mRNA levels for both latent mRNAs were highly correlated with GAPDH ($R^2 = 0.5855$ and $m = 1.14$ for orf72/v-cyclin; $R^2 = 0.5755$ and $m = 0.71$ for orf71/v-FLIP), consistent with the idea that all KS tumor cells transcribe KSHV latent mRNAs and that the majority of cells in an individual KS biopsy are KSHV infected. By contrast, Fig. 3C plots the CT values for K14 and orf22, two KSHV lytic mRNAs, relative to GAPDH. Here, it was not possible to calculate a regression line. Rather two populations of data could be discerned, those with considerable amounts of KSHV lytic mRNAs and those with no detectable level of KSHV lytic mRNAs (CT = 50). This outcome suggests that KS tumors can be stratified according to the degree of lytic reactivation in the tumor.

Discussion

Transcriptional profiling of human tumors yields crucial insights with regard to pathological classification, oncogene discovery, and therapy selection. Its application to routine clinical diagnostics has been limited chiefly by the scarcity of high-quality and high-quantity biopsy material, which is required for hybridization-based arrays. To circumvent this bottleneck in assay sensitivity, we developed a real-time, quantitative, RT-PCR-based array, which covers the entire KSHV genome (5). Here, we applied this methodology to the identification of KSHV mRNAs that are consistently transcribed in primary KS lesions. To date, no cell line that maintains KSHV has been derived from KS lesions, and our study represents the first comprehensive evaluation of KSHV transcription in primary KS lesions, as opposed to culture-adopted PEL cell lines, which may or may not conserve the transcription program of the primary tumor.

Extending earlier observations (2, 12), we found that KSHV LANA, v-cyclin, and v-FLIP mRNAs were present in all KS tumors. The ratio of LANA mRNA to GAPDH mRNA can be used to obtain a quantitative measure of KS tumor cells, rather than surrounding normal stroma, in a given biopsy. Such a measure is important because it will allow us to relate changes in cellular transcription to the degree of latent KSHV infection. Because the LANA protein is required for KSHV episome persistence and proper genome segregation (18–21), its expression is also required in all latently infected cells (KS, PEL, and MCD). Furthermore, LANA exhibits transforming properties (22). KSHV v-cyclin and v-FLIP may also aid KSHV tumorigenesis by inducing aberrant S-phase progression and inhibiting apoptosis, respectively. The mRNAs that encode all three proteins originate from a common, latent viral promoter (12, 13, 23) and in this array are queried by multiple independent primers. Our analysis of primary KS lesions reaffirms LANA as an obligate tumor marker for KSHV-associated malignancies.

A comparison of the KSHV latent gene expression profile in KS (this study) with prior data obtained from PEL cells using the same array (5) expands prior classifications of KSHV latent and lytic genes (5–7, 23, 24): type I latency genes (such as LANA, v-cyclin, and v-FLIP) are transcribed in all KSHV-associated tumors (KS, PEL, and MCD) and are not induced upon KSHV lytic replication. Type I-B latency genes (such as LANA-2/vIRF-3) are transcribed only in KSHV-associated B-cell malignancies and not in endothelial-derived KS tumors and are not induced upon KSHV lytic replication. Type II latency genes (such as K12/kaposin or K9/vIRF-1) are transcribed in KSHV-associated tumors, but their transcription is further enhanced during viral lytic replication. Those genes most likely have a dual function during latent and lytic replication. Finally, type III comprises

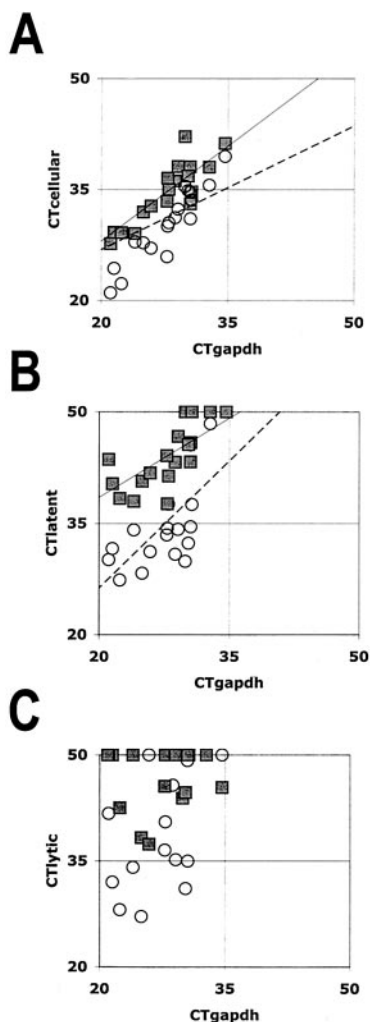


Fig. 3. Regression analysis of individual KSHV mRNAs. Plotted on the vertical axis are the CT values for two cellular mRNAs (A; boxes for c-myc, circles for actin), two KSHV latent mRNAs (B; boxes for v-FLIP/orf71, circles for cyclin/orf72), and two KSHV lytic mRNAs (C; boxes for orf45, circles for K14) relative to the CT value for GAPDH mRNA for each KS sample.

exclusively lytic mRNAs (α , β , and γ -2), which are required for virus propagation.

It is intriguing that the relative levels of KSHV lytic mRNAs segregate KS tumors into two groups (with or without discernable lytic viral transcription) because it implies the possibility that KSHV transcription changes during stages of KS tumor progression. At this point, our collection of KS tumors is too limited to assign a mechanistic role for any one KSHV lytic gene in KS tumor development. Clearly, additional studies are needed, in particular to determine whether specific KSHV lytic mRNAs can predict clinical outcomes or the susceptibility of individual KS lesions to antiviral therapy (25).

The mRNA for KSHV IFN-regulatory factor K9/vIRF-1 was also present in every KS sample, and its transcription profile clustered with the KSHV latency I mRNAs, LANA, v-cyclin, and v-FLIP. K9/vIRF-1 was initially identified because of its sequence homology to cellular IFN-regulatory factors (26–28). It inhibits IFN-mediated signal transduction pathways and transforms NIH3T3 cells in culture, presumably by interfering with p53 function and/or induction of c-myc. Two transcription start sites have been identified for K9/vIRF-1: a site distal to the AUG, which is active during latency in PEL; and a second, more proximal site, which is induced upon lytic reactivation (14). The data presented here establish the presence of K9/

v-IRF-1 in all KS tumors. This strengthens the role of K9/v-IRF-1 in KS tumorigenesis. The homologous LANA-2/vIRF-3 did not cluster with LANA, consistent with earlier reports that showed LANA2/vIRF-3 to be expressed significantly only in PEL and MCD (15). This suggests that the different, redundant, vIRFs are needed in different target cells and/or during different stages of viral infection.

In summary, this study represents the first transcriptome analysis for KSHV in primary KS biopsies. It validates the general applicability of real-time QPCR-based arrays to clinical samples. Real-time QPCR-based arrays for other tumor-associated herpesviruses or select cellular real-time QPCR arrays should have similar sensitivities and utilities. Genome-wide PCR uncovered viral latent genes that were commonly transcribed in all KSHV-associated tumors (LANA, v-cyclin, and v-FLIP). These viral proteins represent highly tumor-specific targets for drug-based or vaccine-based KS therapy. Our analysis also identified two sequence-related and functionally overlapping genes, which were preferentially transcribed during latent infection of either endothelial/mesenchymal lineage cells (K9/vIRF-1 in KS) or lymphoid lineage cells (LANA-2/vIRF-3 in PEL). This points to an essential role for vIRFs in KSHV pathogenesis. Our clustering based on lytic mRNA transcription should be of clinical importance with regard to differential tumor therapy using antiviral drugs.

Acknowledgments

Tumor samples were kindly provided by the ACSB. The author thanks R. Hines-Boykin and Arndt Pechstein for technical help and B. Damania, M. Sakalian, and M. Lagunoff for critical reading of the manuscript.

References

- Antman, K., and Chang, Y. Kaposi's sarcoma. *N. Engl. J. Med.*, 342: 1027–1038, 2000.
- Dupin, N., Fisher, C., Kellam, P., Ariad, S., Tulliez, M., Franck, N., van Marck, E., Salmon, D., Gorin, I., Escande, J. P., Weiss, R. A., Alitalo, K., and Boshoff, C. Distribution of human herpesvirus-8 latently infected cells in Kaposi's sarcoma, multicentric Castlemann's disease, and primary effusion lymphoma. *Proc. Natl. Acad. Sci. USA*, 96: 4546–4551, 1999.
- Cesarman, E., Chang, Y., Moore, P. S., Said, J. W., and Knowles, D. M. Kaposi's sarcoma-associated herpesvirus-like DNA sequences in AIDS-related body-cavity-based lymphomas. *N. Engl. J. Med.*, 332: 1186–1191, 1995.
- Soulier, J., Grollet, L., Oksenhendler, E., Cacoub, P., Cazals-Hatem, D., Babinet, P., d'Agay, M. F., Clauvel, J. P., Raphael, M., Degos, L., et al. Kaposi's sarcoma-associated herpesvirus-like DNA sequences in multicentric Castlemann's disease. *Blood*, 86: 1276–1280, 1995.
- Fakhari, F. D., and Dittmer, D. P. Charting latency transcripts in Kaposi's sarcoma-associated herpesvirus by whole-genome real-time quantitative PCR. *J. Virol.*, 76: 6213–6223, 2002.
- Jenner, R. G., Alba, M. M., Boshoff, C., and Kellam, P. Kaposi's sarcoma-associated herpesvirus latent and lytic gene expression as revealed by DNA arrays. *J. Virol.*, 75: 891–902, 2001.
- Paulose-Murphy, M., Ha, N. K., Xiang, C., Chen, Y., Gillim, L., Yarchoan, R., Meltzer, P., Bittner, M., Trent, J., and Zeichner, S. Transcription program of human herpesvirus 8 (Kaposi's sarcoma-associated herpesvirus). *J. Virol.*, 75: 4843–4853, 2001.
- Eisen, M. B., Spellman, P. T., Brown, P. O., and Botstein, D. Cluster analysis and display of genome-wide expression patterns. *Proc. Natl. Acad. Sci. USA*, 95: 14863–14868, 1998.
- Yuen, T., Wurmbach, E., Pfeffer, R. L., Ebersole, B. J., and Sealfon, S. C. Accuracy and calibration of commercial oligonucleotide and custom cDNA microarrays. *Nucleic Acids Res.*, 30: e48, 2002.
- Pfaffl, M. W., Horgan, G. W., and Dempfle, L. Relative expression software tool (REST) for group-wise comparison and statistical analysis of relative expression results in real-time PCR. *Nucleic Acids Res.*, 30: e36, 2002.
- Pfaffl, M. W. A new mathematical model for relative quantification in real-time RT-PCR. *Nucleic Acids Res.*, 29: e45, 2001.
- Dittmer, D., Lagunoff, M., Renne, R., Staskus, K., Haase, A., and Ganem, D. A cluster of latently expressed genes in Kaposi's sarcoma-associated herpesvirus. *J. Virol.*, 72: 8309–8315, 1998.
- Jeong, J., Papin, J., and Dittmer, D. Differential regulation of the overlapping Kaposi's sarcoma-associated herpesvirus (KSHV/HHV-8) vGCR (orf74) and LANA (orf73) promoter. *J. Virol.*, 75: 1798–1807, 2001.
- Chen, J., Ueda, K., Sakakibara, S., Okuno, T., and Yamanishi, K. Transcriptional regulation of the Kaposi's sarcoma-associated herpesvirus viral interferon regulatory factor gene. *J. Virol.*, 74: 8623–8634, 2000.

15. Rivas, C., Thlick, A. E., Parravicini, C., Moore, P. S., and Chang, Y. Kaposi's sarcoma-associated herpesvirus LANA2 is a B-cell-specific latent viral protein that inhibits p53. *J. Virol.*, *75*: 429–438, 2001.
16. Lubyova, B., and Pitha, P. M. Characterization of a novel human herpesvirus 8-encoded protein, vIRF-3, that shows homology to viral and cellular interferon regulatory factors. *J. Virol.*, *74*: 8194–8201, 2000.
17. Vandesomepele, J., De Preter, K., Pattyn, F., Poppe, B., Van Roy, N., De Paepe, A., and Speleman, F. Accurate normalization of real-time quantitative RT-PCR data by geometric averaging of multiple internal control genes. *Genome Biol.*, *3*: RESEARCH0034, 2002.
18. Cotter, M. A., II, and Robertson, E. S. The latency-associated nuclear antigen tethers the Kaposi's sarcoma-associated herpesvirus genome to host chromosomes in body cavity-based lymphoma cells. *Virology*, *264*: 254–264, 1999.
19. Ballestas, M. E., Chatis, P. A., and Kaye, K. M. Efficient persistence of extrachromosomal KSHV DNA mediated by latency-associated nuclear antigen. *Science (Wash. DC)*, *284*: 641–644, 1999.
20. Hu, J., Garber, A. C., and Renne, R. The latency-associated nuclear antigen of Kaposi's sarcoma-associated herpesvirus supports latent DNA replication in dividing cells. *J. Virol.*, *76*: 11677–11687, 2002.
21. Lim, C., Sohn, H., Lee, D., Gwack, Y., and Choe, J. Functional dissection of latency-associated nuclear antigen 1 of Kaposi's sarcoma-associated herpesvirus involved in latent DNA replication and transcription of terminal repeats of the viral genome. *J. Virol.*, *76*: 10320–10331, 2002.
22. Radkov, S. A., Kellam, P., and Boshoff, C. The latent nuclear antigen of Kaposi sarcoma-associated herpesvirus targets the retinoblastoma-E2F pathway and with the oncogene hras transforms primary rat cells. *Nat. Med.*, *6*: 1121–1127, 2000.
23. Sarid, R., Flore, O., Bohenzky, R. A., Chang, Y., and Moore, P. S. Transcription mapping of the Kaposi's sarcoma-associated herpesvirus (human herpesvirus 8) genome in a body cavity-based lymphoma cell line (BC-1). *J. Virol.*, *72*: 1005–1012, 1998.
24. Zhong, W., Wang, H., Herndier, B., and Ganem, D. Restricted expression of Kaposi sarcoma-associated herpesvirus (human herpesvirus 8) genes in Kaposi sarcoma. *Proc. Natl. Acad. Sci. USA*, *93*: 6641–6646, 1996.
25. Martin, D. F., Kuppermann, B. D., Wolitz, R. A., Palestine, A. G., Li, H., and Robinson, C. A. Oral ganciclovir for patients with cytomegalovirus retinitis treated with a ganciclovir implant. Roche Ganciclovir Study Group. *N. Engl. J. Med.*, *340*: 1063–1070, 1999.
26. Zimring, J. C., Goodbourn, S., and Offermann, M. K. Human herpesvirus 8 encodes an interferon regulatory factor (IRF) homolog that represses IRF-1-mediated transcription. *J. Virol.*, *72*: 701–707, 1998.
27. Li, M., Lee, H., Guo, J., Neipel, F., Fleckenstein, B., Ozato, K., and Jung, J. U. Kaposi's sarcoma-associated herpesvirus viral interferon regulatory factor. *J. Virol.*, *72*: 5433–5440, 1998.
28. Jayachandra, S., Low, K. G., Thlick, A. E., Yu, J., Ling, P. D., Chang, Y., and Moore, P. S. Three unrelated viral transforming proteins (vIRF, EBNA2, and E1A) induce the MYC oncogene through the interferon-responsive PRF element by using different transcription coadaptors. *Proc. Natl. Acad. Sci. USA*, *96*: 11566–11571, 1999.